Anomalous concentration dependence of the ^{119}Sn Mössbauer isomer shift of Ag-Sn alloys

1998 J. Phys.: Condens. Matter 10 8573

(http://iopscience.iop.org/0953-8984/10/38/017)

J. Phys.: Condens. Matter **10** (1998) 8573–8586. Printed in the UK PII: S0953-8984(98)94405-8

Anomalous concentration dependence of the ^{119}Sn Mössbauer isomer shift of Ag–Sn alloys

H Shechter†, D Haskel‡‖, E A Stern‡ and Y Yacoby§

† Solid State Institute, Technion, Haifa, Israel

‡ Physics Department, Box 351560, University of Washington, Seattle, WA 98195, USA

§ Racah Institute of Physics, Hebrew University, Jerusalem, Israel

Received 19 May 1998, in final form 10 July 1998

Abstract. The position of the $E_\gamma \approx 24$ keV Mössbauer resonant absorption line of ^{119}Sn was measured at various temperatures and concentrations of substitutional Sn impurities in the α-phase of the Ag–Sn alloy. Whereas 1.0 and 2.0 at.% Sn alloys showed the expected temperature dependence of the line shift (LS), 4.0 and 8.0 at.% Sn alloys showed several anomalous features. After aging at room temperature (RT) for several months, these alloys showed hysteresis of the LS from RT up to about 500 K. At about 520 K, the unusual slope transforms to its expected value but continues with an increased *isomer shift* (IS). Further thermal cycles resulted in the expected slope of the LS with no measurable hysteresis, except for the transition region around 520 K above which the IS increase persisted. The experiments indicate that after thermal cycling the high-concentration alloys are in an intermediate state below about 500 K, which becomes metastable at RT as shown by the changes with aging. The transition to the increased-IS state at $T \approx 520$ K, however, is independent of the thermal history. A discussion of the observed phenomena is presented, which is based on thermally induced changes in the Sn–Sn distribution (short-range order) that preserve the long-range order of the alloy.

1. Introduction

The question of local stability around impurities in solid solutions of binary alloys has been the focus of many recent investigations [1–8]. For many alloys the addition of a small amount of impurity has profound effects on their mechanical, electronic and vibrational properties. Even though a great deal of knowledge has been accumulated on the macroscopic properties of many alloys, microscopic information on the electronic and dynamical state of these impurities as well as on their interactions, which is crucial in determining the origin of the macroscopic properties, is scarce. Accessing this information requires techniques that can selectively tune to the impurity atoms in order to distinguish them from the background of majority host atoms. Mössbauer spectroscopy is particularly suitable for this purpose.

In the present case the parameters obtained from Mössbauer spectroscopy on substitutional Sn impurities in Ag are

(a) the resonance energy position,
(b) the intensity of the spectral line and
(c) the resonance linewidth [9].

These parameters are determined simultaneously and extracted from the spectra by a standard non-linear least-squares minimization procedure.

‖ E-mail: haskel@phys.washington.edu.

0953-8984/98/388573+14$19.50

The position of the Mössbauer resonance or line shift (LS) is mainly determined by the differences in local electronic configuration of Sn atoms in the source and absorber, the isomer shift (IS) $\Delta E_{\rm IS}$ [10]. In addition, relativistic effects on the resonance position such as the second-order Doppler shift (SODS) lead to a reduction of the recoilless photon's energy by

$$\Delta E_{\rm SODS} = -\frac{\langle v^2 \rangle}{2c^2} E_\gamma \tag{1}$$

where $\langle v^2 \rangle$ is the mean squared velocity of the Sn impurities along the direction of the emitted/absorbed photon, $\hat{\boldsymbol{u}}$ ($\langle v^2 \rangle = \langle (\boldsymbol{v} \cdot \hat{\boldsymbol{u}})^2 \rangle$), and c is the velocity of light [11]. It can be shown [12] that in the harmonic approximation and high-temperature limit $T \geqslant \frac{1}{2}\theta_{\rm eff}$ ($\theta_{\rm eff}$ is a characteristic temperature for the impurity atom simply related to the interaction potential of the impurity and its neighbouring atoms), $\langle v^2 \rangle$ becomes independent of the local bonding forces and depends only on the mass of the impurity M_i, resulting in (reference [12])

$$\Delta E_{\rm SODS} = -\frac{3k_B E_\gamma}{2M_i c^2}(T_a - T_s) \tag{2}$$

with k_B Boltzmann's constant and $T_{a,s}$ the temperatures of the absorber and source nuclei, respectively.

The total line shift observed is then

$$\Delta E_{\rm LS} = \Delta E_{\rm IS} + \Delta E_{\rm SODS}. \tag{3}$$

With no magnetic or electric hyperfine splitting of the nuclei levels in either the source or the absorber, the determination of the spectral LS is quite easy. Usually it is sufficient to fit a single Lorentzian to the data (for thin absorbers).

Different mechanisms can contribute to the broadening of the resonance linewidth, Γ, such as saturation effects due to thick absorbers [13, 14], diffusion of the impurity atoms [15] and local inhomogeneities of electric field gradients causing unresolved quadrupole splitting [16]. For sufficiently thin absorbers a change of $\Gamma/100$ in the resonance line position can be detected.

In previous reports [17, 18] we described some dynamical properties of Sn impurities in Pb and Ag hosts: in particular, in figure 5 of reference [17] we reported on the temperature dependence of the LS for 2.0, 4.0 and 8.0 at.% Sn in a Ag host; all of the concentrations were below the limit of Sn solubility in Ag ($\approx$11.3 at.% at 724 °C and 9.35 at.% at 218 °C [19]). Anomalous behaviour in the LS can be seen in figure 5 (reference [17]) for samples with 4.0 and 8.0 at.% Sn in Ag. It is manifested, for virgin samples, in a deviation of the slope from the expected value given by equation (2), together with a rather sharp increase in IS at about $T \approx 520$ K. The anomalous deviation in slope disappears after the first heating–cooling cycle while the change in IS at $T \approx 520$ K, as detailed below, persists and is independent of the thermal history of the sample. The motivation of the present work is the wish to investigate this anomalous behaviour and try to elucidate the mechanism by means of which it takes place.

2. Experimental details and results

2.1. Sample preparation

The samples were made of 99.999% pure Ag pellets and Sn powder enriched to 84% with the ^{119}Sn isotope (natural Sn contains $\sim$8% ^{119}Sn). The enriched Sn powder was obtained by reducing enriched SnO_2 powder under a H_2 atmosphere at 1200 K for one hour. The

correct mixture of components was made up, having a total mass between 2.5 and 10 grams, and put in a quartz ampoule which was then evacuated using a mechanical pump and sealed. The samples were held in a furnace at least 50 degrees Kelvin above the melting temperature of pure Ag for 24 hours, and then quenched into cold water.

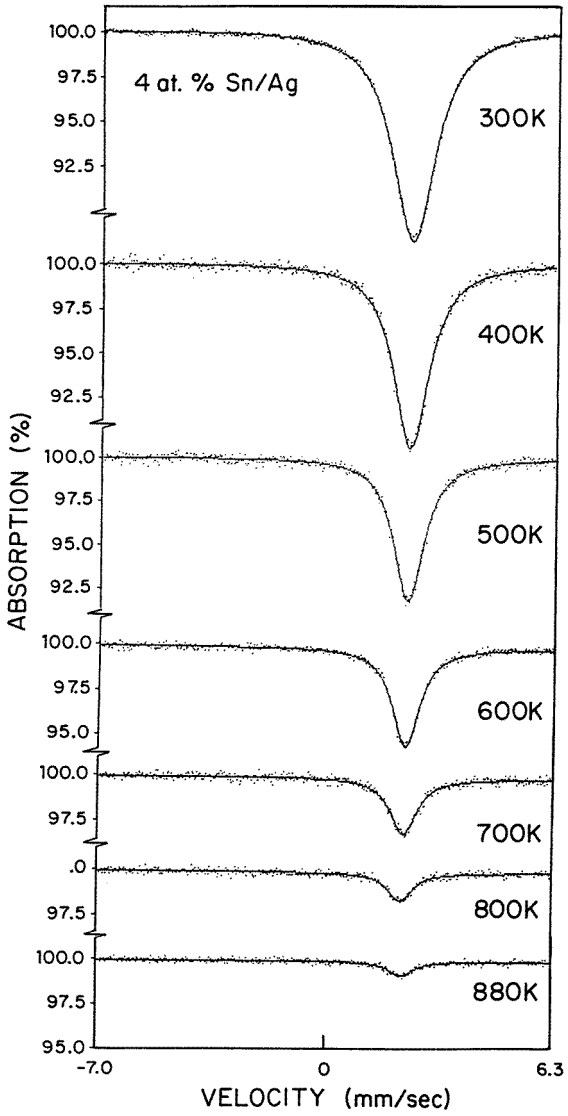

Figure 1. Mössbauer spectra for 4.0 at.% enriched Sn in Ag at various temperatures. A single Lorentzian line was used to obtain the line position, linewidth at half-maximum and total area in each case.

The ingot was then extracted and cold-rolled into a foil. The final thickness of the foil was required to be such that the sample would be about one absorption length ($\mu x \sim 1$) thick for non-resonant 24 keV γ-rays. This resulted in a sample thickness of about $t \approx 100$ μm for the 1.0, 2.0 and 4.0 at.% Sn samples. The 8.0 at.% Sn sample was rolled down to

$t \approx 35$ μm, to keep the saturation effects in the resonance line within the linear regime, for which Γ is proportional to the absorber 'effective' thickness [13, 14, 20]. Following the rolling, the samples were annealed in evacuated quartz ampoules at about 100 degrees Kelvin below their melting temperatures for about 48 hours.

The relative Sn concentrations in our alloys were confirmed by Auger spectroscopy (AS) and EDS (energy-dispersive spectroscopy). AS gave the ratio for the 1.0, 2.0 and 4.0 at.% Sn alloys as 1:1.6:4.7; EDS gave 1:2.1:3.2 for the same alloys.

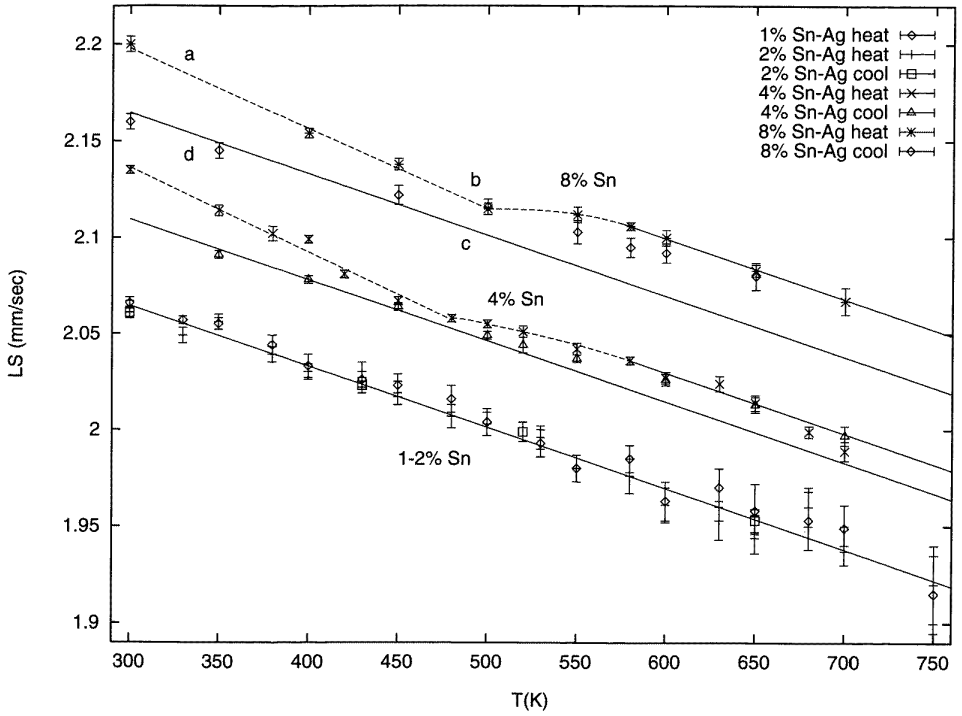

Figure 2. Plots of the line shift versus T for alloys containing 1.0, 2.0, 4.0 and 8.0 at.% of enriched Sn, which were aged for several months at RT. The vertical scale is displaced upward by 0.05 and 0.12 mm s^{-1} for the 4.0 and 8.0 at.% samples, respectively. Solid lines correspond to the theoretical value of the SODS given in equation (2) while dashed lines are guides to the eye.

2.2. Spectroscopy

The Mössbauer measurements were performed with the alloys as the fixed absorber versus a moving source in a constant-acceleration mode. The source was ^{119m}Sn in a $CaSnO_3$ matrix with linewidth $\Gamma_s = 0.382$ mm s^{-1} (the natural linewidth is 0.32 mm s^{-1}). The velocity scale was calibrated against the quadrupole splitting of SnF_2 [21]. The Ag:Sn samples were heated to the desired temperatures and kept stable to within 0.5%. It was important to keep the temperature constant for the long run-time required to acquire a minimum of 10^6 counts (0.1% statistical noise-to-signal ratio), which was up to two days for the lowest concentrations and highest temperatures, due to the low Mössbauer fraction coupled with the low Sn content.

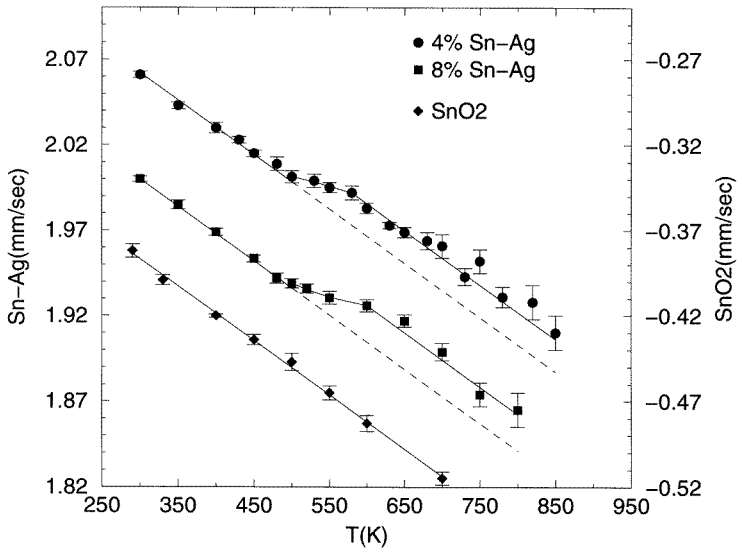

Figure 3. Plots of the line shift versus T for alloys containing 4.0 and 8.0 at.% of enriched Sn measured after the first heating–cooling cycle was completed. The 8.0 at.% data were displaced downward by 0.05 mm s^{-1} for clarity. SnO_2 is also shown for comparison. Lines through the experimental points correspond to the SODS slope given by equation (2), except in the transition interval around $T \approx 520$ K.

Figure 1 shows typical spectra for 4.0 at.% enriched Sn in Ag at different values of T. The solid curve through the data points represents a Lorentzian best fit to the data. The analysis yields the spectral intensity, line position and linewidth. Attempts to fit more than one Lorentzian resulted in poorer fits. For evaluation of the effective absorber thickness we used a procedure described before [17]. Extrapolation to zero thickness gives an absorber linewidth of $\Gamma_a = 0.44$ mm s^{-1}. The 'intrinsic' broadening in our alloys of $\sim$0.12 mm s^{-1} could result from the tails of the Friedel oscillations in the shielding charge around the tin impurities causing unresolved quadrupole splitting [16] or varying IS due to the charge variations. This is consistent with our observation of a smaller 'intrinsic' broadening for Pb–Sn alloys [17], in which weaker tails are expected since Sn and Pb have the same valence charge.

Figure 2 shows the temperature dependence of the LS obtained by a first cycling of different alloys which have been aged at RT for several months. The behaviour of the 1.0 and 2.0 at.% Sn alloys is as expected from the temperature-dependent SODS described by equation (2) and showed reversibility in the heating–cooling cycle. The 4.0 and 8.0 at.% Sn alloys, however, initially showed a bigger slope than that expected from equation (2) up to about $T \approx 500$ K, where a sudden increase in IS is observed together with a change in slope to a value consistent with equation (2). Cooling resulted in significant hysteresis below $T \approx 500$ K.

Figure 3 displays the temperature dependence of the LS for the 4.0 and 8.0 at.% samples measured after the first cycle was completed. The slope is as expected from equation (2) and no detectable hysteresis was found in the heating–cooling process. The LS measured for powder SnO_2 is also shown for comparison. For these alloys, a change in IS is observed at around $T \approx 520$ K, indicating a change in the electronic charge density at the Sn nucleus. This change was found to be reproducible in further cycles, as was its reversibility. The

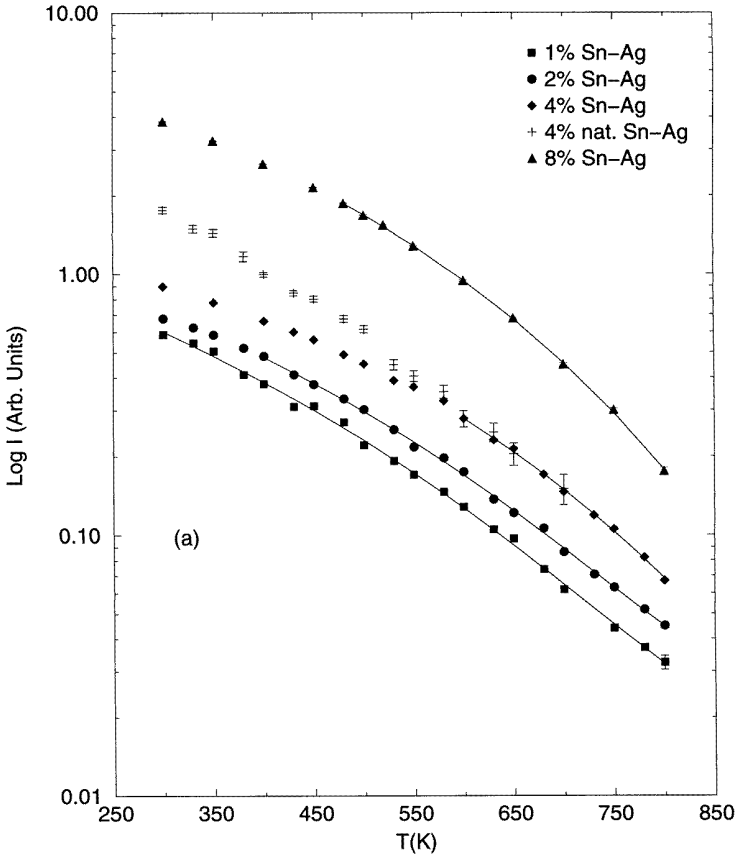

Figure 4. (a) Plots of log I versus T. The vertical scale of the 4.0 and 8.0 at.% data is displaced for clarity. The solid lines are fits to experimental data made using an anharmonic model. The fitting was performed over a temperature range in which the samples are 'thin', as determined from the linewidth behaviour. (b) Plots of the linewidth Γ versus T for the different alloys.

results for the alloys with 1.0 and 2.0 at.% Sn were no different for the first and second cycles.

Over the temperature range presented here, the temperature dependence of the spectral intensity, as shown in figure 4(a), is as expected for lattice vibrations of the Sn impurities, in a slightly anharmonic potential. Excess absorber thickness, in addition to causing line broadening (see figure 4(b)), decreases the spectral intensity I, as can be seen by comparing the two alloys containing 4% natural Sn and 4% enriched Sn. No anomalous behaviour was observed in the intensity over this range of temperatures for any of the alloys, and the same T-dependence was obtained for all cycles.

3. Discussion

We separate our discussion into consideration of (A) the hysteretic abnormal slope of the LS versus temperature observed after aging (figure 2) and (B) the shift in the IS above 520 K (figure 3) found for the 4.0 and 8.0 at.% Sn samples.

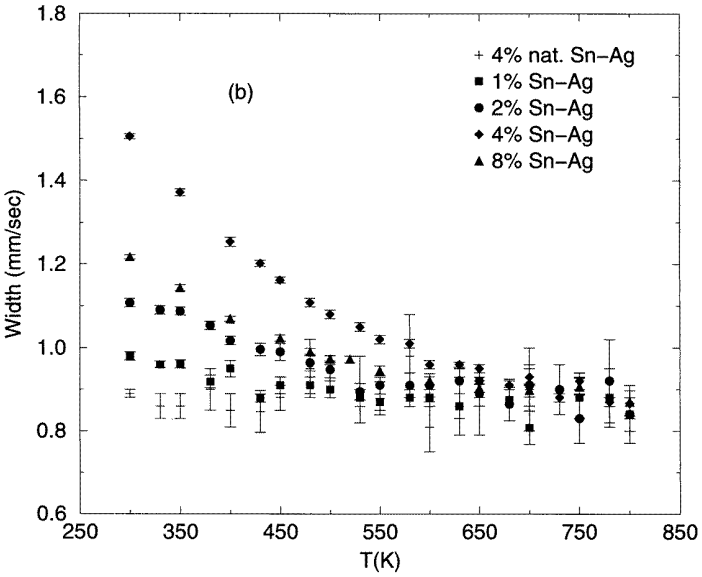

Figure 4. (Continued)

3.1. Hysteresis

We first direct our attention to the irreversible LS observed for the 4.0 and 8.0 at.% Sn samples after they have been aged for several months at RT. We associate the initial abnormal slope of the curve on heating (a $\rightarrow$ b, figure 2) and the subsequent hysteresis on cooling (c $\rightarrow$ d, figure 2) with atomic rearrangements from an equilibrium state into an intermediate state which persists through the Mössbauer measurements period. At RT the intermediate state is metastable and on aging it approaches its equilibrium state.

As shown in figure 2, hysteresis effects on the LS were detected only for the more concentrated samples and not for the 1.0 and 2.0 at.% Sn samples. This hysteresis becomes apparent for samples with Sn concentrations somewhere between 2.0 and 4.0 at.% (see figure 5). When sufficient time is allowed (of the order of several months at RT), the Sn impurities in the 4.0 and 8.0 at.% Sn alloys rearrange in a way that increases the electronic charge density at the Sn site (an increase in IS corresponds to an increase in charge density at the nucleus as can be seen from the difference in LS between SnO_2 and metallic β-Sn: -0.38 mm s^{-1} and 2.54 mm s^{-1} relative to $CaSnO_3$ at RT, respectively).

The temperature-induced rearrangement of Sn atoms leads to an intermediate state over the temperature region 300 K $\leqslant T \leqslant$ 500 K, as seen by the presence of hysteresis. This new metastable state is probably characterized by a Sn–Sn configuration similar to that in the 1.0 and 2.0 at.% Sn alloys, as can be seen from the monotonic dependence on the concentration of Sn of the RT LS of the 1.0, 2.0, and cycled 4.0 and 8.0 at.% Sn alloys (figure 5). The decrease of the LS with the Sn content in the lower curve of figure 5 can be understood by considering the linear lattice expansion introduced with doping causing a reduction in electron density at the Sn nuclei. For these alloys, the relative increase in lattice parameter reaches about 1% at 8.0 at.% Sn [22].

Beside the concentration dependence of the LS, changes in the effective potential sensed by the Sn atoms are evident in the concentration dependence of the resonance's intensity, shown in figure 4(a). The values obtained for θ_{eff} by fitting $\ln I$ versus T curves over the

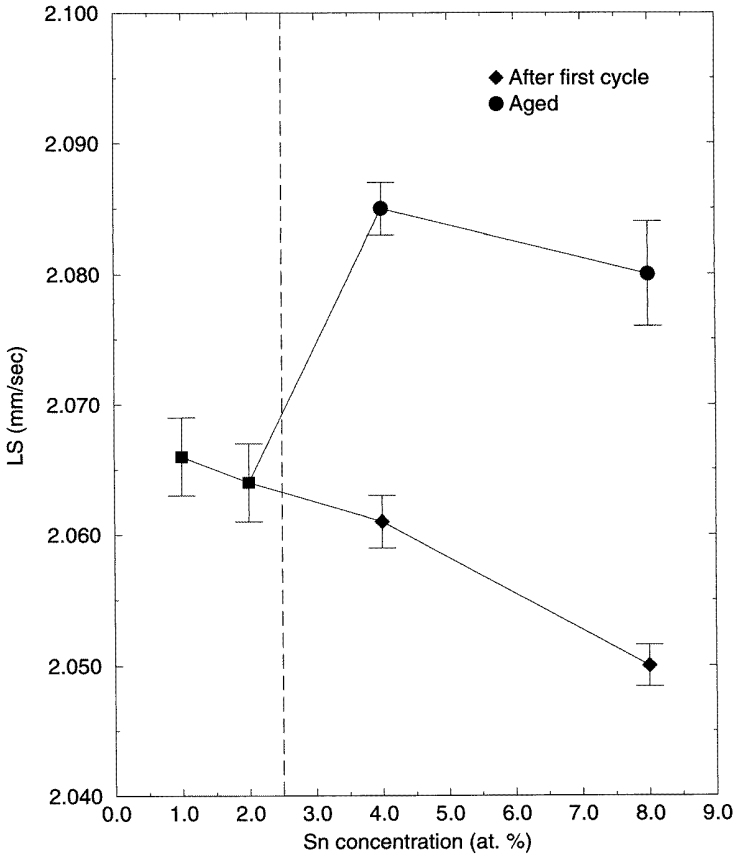

Figure 5. Measured line shifts at RT for aged and cycled alloys. The dashed line indicates where the interaction between Sn atoms becomes noticeable in our measurements. The results for 1.0 and 2.0 at.% Sn alloys are no different for initial and further cycles. Solid lines are guides to the eye.

range [300, 500] K to a first-order polynomial in T are 195(3) K, 195(5) K and 185(5) K for the 1.0, 2.0 and 4.0 at.% Sn samples, respectively. We also studied a sample containing 4.0 at.% natural (non-enriched) Sn to correct for intensity saturation effects in the sample containing enriched Sn [13] (we do not have such a measurement for the 8 at.% sample). This result shows a similar change in the effective potential of the Sn atoms for Sn contents between 2.0 and 4.0 at.%.

Our measurements of θ_{eff} are in agreement with previous results on these alloys. Bryukhanov *et al* [23] found $\theta_{\mathrm{eff}} = 207(15)$ K for Sn concentrations over the range 1.0–3.0 at.% by intensity measurements over the temperature range [77, 300] K. No concentration dependence of the Mössbauer parameters was found over this range. Balkashin and Chekin [24] reported $\theta_{\mathrm{eff}} = 200(3)$ K for 1.0 at.% Sn in Ag, by measuring the intensity for temperatures over the [4.2, 350] K range, with θ_{eff} decreasing for higher concentrations down to 182(3)K for 9.0 at.% Sn. More recently Andreasen *et al* [25] found $\theta_{\mathrm{eff}} = 190(8)$ K for very dilute Sn concentrations, of about 10^{13} Sn atoms per cm^2 (our samples have approximately 10^{18} Sn atoms per cm^2).

These results indicate that for Sn concentrations below ≈3.0 at.%, the electronic and

vibrational properties of the Sn are nearly independent of concentration. For higher Sn contents, changes in these properties are observed.

The observed concentration dependence of the RT IS of the aged samples (figure 5) cannot be explained by an increased electron density at a Sn atom simply due to the increased concentration of neighbouring Sn atoms without some additional change. If no phase transition occurs, one expects this effect to show no hysteresis with temperature. However, we do find hysteresis in the aged RT LS, excluding this possible explanation.

Temperature dependence of the LS beyond the SODS with hysteresis is observed at structural phase transitions in which the environment of the impurity atoms changes. No structural phase transition which affects the long-range order in the atomic arrangement is known to occur for these alloys in the range of temperatures and concentrations studied here. However, the distribution of the Sn impurities over the lattice sites, i.e. their SRO, may change with temperature through diffusion. In a close-packed structure such as fcc, the diffusion mechanism is mainly via vacancies and thus is strongly dependent on vacancy concentration. At low temperatures, the contribution of the configurational entropy term to the Gibbs free energy, $F = E - TS$, is small, and the free energy of the alloy is dominated by the energy of the interaction between the alloy's components. If the impurities interact with each other, the Sn atoms will have a preferential SRO configuration to which local probes such as the Mössbauer effect, nuclear magnetic resonance (NMR) and x-ray absorption fine structure (XAFS) will be sensitive. At higher temperatures, the free-energy contribution of configurational entropy becomes important and increasing of the entropy by randomization of the mixture will occur, leading to a loss of SRO (provided that contributions to the entropy other than the configurational entropy are small). Since randomization happens through diffusion, it will be observed only when the diffusion is fast enough compared to the experimental/observational time.

Garlipp *et al* [26] studied SRO effects in Ag–Sn alloys by means of electrical resistivity measurements. In these particular alloys, an increase in SRO is accompanied by a decrease in electrical resistivity. They measured samples with 3.0, 5.0 and 7.0 at.% Sn content after 15 minutes of isochronal annealing over a temperature range [300, 550] K, with ten-degree intervals. If no SRO effects are present, resistivity should steadily increase with temperature. This was indeed observed for the 3.0 at.% Sn alloy. However, they discovered a moderate decrease in slope for the alloy with 5.0 at.% Sn at about 400 K and a much bigger change was found for the 7.0 at.% sample at about 430 K. The decrease in resistivity at intermediate temperatures indicated an *increase* in SRO with temperature. If the mobility of the Sn atoms increases for lower Sn contents, SRO will be reached at lower temperatures. Garlipp *et al* concluded that only the 7.0 at.% sample shows a measurable SRO effect, and whether such effects exist in the 5 at.% sample was not clear from the measurements.

The Mössbauer LS is even more sensitive to SRO effects, since it directly probes the impurity environment. Figure 2 shows a behaviour similar to that obtained in the resistivity studies. The initial slope (a $\rightarrow$ b) can be attributed to Sn atoms being in a SRO equilibrium state obtained when the samples are stored at RT for several months. For dilute solutions of Sn in Ag, the diffusion coefficient is [27] $D = 0.25\exp(-39\,300/\mathrm{RT})$. At an equilibrium concentration of vacancies, this means that at 400 K the Sn atoms are able to move through a distance of $\sim$0.1 Å during the run time of 6–7 h at each temperature point. At 500 K they move by $\sim$18 Å. It is then possible that if the Sn impurities interact with each other, a change in their SRO can be completed during the sampling time at temperatures around 500 K, causing a change in the measured IS. When cooling (c $\rightarrow$ d, figure 2), the metastable disordered state is frozen in (hysteretic behaviour) until sufficient time has been allowed for the system to relax into the equilibrium, ordered state at low temperatures.

These results are in qualitative agreement with the resistivity studies of Garlipp *et al* [26]. We therefore conclude that the anomalous change in slope is caused by a SRO phase transition where changes in only the *local* configuration of the Sn atoms occur but otherwise do not affect the long-range order of the crystal.

3.2. Reversible behaviour

Figure 3 shows the temperature dependence of the LS for the samples with higher concentrations when thermally cycled for the second time and further; for the lower concentrations no differences were detected between first and further cycles. As mentioned before, the cycled 4.0 and 8.0 at.% samples have an intermediate state for $300 \lesssim T \lesssim 500$ K which persists during the measurements. Our measurements of SnO_2 are also shown for comparison. First we note that the slopes are the same for the three samples and correspond well to the value expected from equation (2).

However, at $T \approx 520$ K, a change occurs involving a shift from the otherwise linear dependence on T of the LS. The transition is completed within a rather narrow range of temperature (about fifty degrees) after which the slope returns to its expected value and a shift in IS (SIS) of $\Delta E_{SIS} = 0.02$ mm s^{-1} occurs which corresponds to $\sim\Gamma/30$, or an energy change of about 10^{-9} eV out of 24 keV! No hysteresis was observed within the sensitivity of our measurements, indicating that the two impurity states are reversible during the measurement time of several hours. It is important to note that the rather sharp SIS shown in figure 3 appears to be present in the aged samples (figure 2) in the same interval of temperatures, but is less noticeable as it is masked by the hysteresis occurring only in the first thermal cycle after aging. The solid lines in figure 2 correspond to the slope predicted by equation (2).

For temperatures at, and above, the SIS ($500 \text{ K} \leqslant T \leqslant 800$ K for samples with 4.0 and 8.0 at.% Sn), no unusual behaviour was observed in the temperature dependence of the intensity or linewidth. Anharmonic contributions to the mean squared displacement of the Sn atoms become significant above about 600 K, as indicated by the deviation of the intensity from the linear behaviour of the harmonic model. However, the manifestation of anharmonicity is gradual with temperature and cannot explain the rapid increase in IS. The linewidth remains constant throughout.

One of the several hypotheses that we first tested as a possible explanation of the observed SIS shown in figure 3 was the presence of precipitates of Sn impurities in clusters: Sn melts at $T \approx 505$ K, in the same region where we observed the unexpected shift.

The occurrence of Sn clusters in our samples is very unlikely. The solubility limit of Sn in Ag is ≈11.3 at.% at 724 °C and 9.35 at.% at 218 °C [19]. Any reasonable extrapolation to RT will give a value greater than 8.0 at.%. The absolute value of the LS found in our samples at RT (LS ≈ 2.06 mm s^{-1}) corresponds to Sn impurities dissolved in Ag. For comparison, Andreasen *et al* [25] reported LS = 2.10(3) mm s^{-1} for very dilute solutions of Sn in Ag. Bryukhanov *et al* found LS = 2.02(2) mm s^{-1} for SnAg alloys with 1.0–3.0 at.% Sn content (all of the LS values are relative to $CaSnO_3$). On the other hand, the LS for metallic β-Sn is LS = 2.542(5) mm s^{-1} at RT [28]. The measured LS is then at variance with those of tin precipitates of appreciable size. If melting of Sn clusters was responsible for the observed shift, the disappearance at $T \approx 520$ K of a line component at ≈2.5 mm s^{-1} would cause a shift to smaller velocity values, whereas the opposite is observed. In addition, the Mössbauer recoilless fraction of β-Sn is so small (≈0.05 at RT) that such clusters would already have almost no effect on the spectra even at RT.

Precipitation of impurities at grain boundaries was also considered as a possible

mechanism. The environment of the Sn atoms at the grain boundaries might be slightly different to that in the bulk. Thermally activated precipitation of Sn atoms in or out of the boundaries could result in a small change in IS.

There are several fundamental problems with that hypothesis. First, for binary alloys with impurity solubility limits of the order of 10%, the solute segregation coefficient K at the grain boundaries is $\sim$10 ($c_b = Kc$, where c_b is the solute concentration at the grain boundaries and c is that in the bulk) [29]. A grain size study of our samples determined a typical size of about 10 μm. For a grain boundary width of about 10 Å, the grain boundary fractional volume is about 3×10^{-4}. With a segregation factor of 10, less than 0.5% of the Sn impurities reside at grain boundaries, and hence the effect that we observe must be a bulk effect. In addition, self-diffusion measurements [30] on polycrystalline Ag–Sn alloys, with Sn concentrations in the range 0.02–6.0 at.%, showed that the Sn segregation coefficient *decreases* as the Sn content increases, meaning that if segregation at grain boundaries is behind the change in IS, the effect should be bigger for the lower concentrations. However, just the opposite is observed, ruling out grain boundaries as the mechanism for explaining the observed change.

The formation of impurity–vacancy (I–V) complexes, whose concentration could depend on temperature [31], was considered. The equilibrium vacancy concentration for a 3.91 at.% Sn–Ag alloy at $T \approx 500$ K, as obtained by extrapolating high-temperature measurements, is $c_V \approx 5 \times 10^{-8}$ [32]. Even in the presence of an attractive impurity–vacancy interaction, the fraction of Sn atoms involved in I–V complexes is $\approx 10^{-6}$. The contribution of Sn atoms in I–V complexes is therefore expected to be negligible in our measurements. In addition, as the concentration of vacancies increases almost linearly with Sn [32] (at least up to $\approx$4.0 at.% Sn), the fraction of Sn atoms in I–V complexes should be nearly independent of concentration. The strong concentration dependence observed here is in disagreement with the predictions of this model.

The SIS in figure 3 indicates an increase in electronic density at the Sn nuclei at around $T \approx 520$ K. Whether the new equilibrium state corresponds to a static, local, change in the equilibrium position of the Sn nuclei or a dynamical state cannot be decided solely on the basis of the results given here. The Mössbauer measurement has an intrinsic characteristic timescale, determined by the lifetime of the excited ($E = 23.875$ keV) nuclear level, $\tau_M \sim 2.6 \times 10^{-8}$ s for ^{119}Sn. The Mössbauer measurement therefore gives a temporal average of the state of the Sn nuclei over the period τ_M. If the new state is dynamic, techniques with longer (e.g., NMR) or shorter (e.g., XAFS) characteristic timescales would lead to different answers for the local environment of Sn atoms. If the new state involves a static distortion, the different techniques should give similar answers [33]. It is therefore of importance to perform such measurements to definitely resolve the nature of the transition shown in figure 3.

3.3. The unified model

An interesting correlation is that the change in IS on aging at RT seen in figure 5 is similar to the change in IS at about $T \approx 520$ K for the samples with the highest concentrations seen in figures 2 and 3, i.e., an extrapolation of the high-temperature behaviour using the expected temperature dependence of the SODS as predicted by equation (2) coincides, within uncertainties, with the RT LS after aging. This suggests that the aged RT samples have a similar SRO to that in their corresponding high-temperature configurations, a phase which we denote by P_2, and therefore that the intermediate phase between RT and 500 K is a different phase. However, this intermediate phase appears to be similar to the equilibrium

phase existing at concentrations below about 3 at.% Sn, which we denote by P_1, on the basis of the continuity of the concentration dependence of the LS as seen in figure 5. The different values of the LS in P_1 and P_2 suggest that the arrangement of the Sn impurities relative to one another changes, with an increase in the number of Sn–Sn neighbours in the P_2 phase. However, somewhat above RT, the P_2 phase becomes unstable relative to the P_1 phase, while above about 520 K the P_2 phase again becomes stable. Thus there appears to be a re-entrant behaviour of the P_2 phase above about 520 K. This is consistent with the resistivity studies of Garlipp *et al* [26] which showed a decrease in randomness (increased SRO) at intermediate temperatures relative to those of the lower- and higher-temperature phases.

As is always the case in re-entrant phase transitions, the intermediate P_1 phase is characterized by a lower free energy (relative to that of the P_2 phase at RT) in the temperature region between somewhat above RT and about 520 K, making it more favourable, but by a higher free energy relative to that of the re-entrant P_2 phase at high temperature. As the configurational contribution to the entropy is expected to result in increased randomness of the solid solution at high temperature, a more ordered (smaller-configurational-entropy) intermediate phase requires either a decrease in internal energy (due to the interaction between the Sn atoms) or an increase in entropy with an origin other than configurational—e.g., vibrational entropy. Whereas we do not have enough information from our measurements to infer the origin of the decreased free energy in the intermediate phase P_1, the behaviour shown by the lower curve of figure 5 indicates that the *configurational* contribution to the entropy in the P_1 phase must resemble those of the 1.0 and 2.0 at.% Sn alloys.

When the sample is cooled from high temperature, it makes a transition from the P_2 to the P_1 phase at 520 K. With further cooling, the diffusion rate becomes so slow that when the low-temperature boundary between P_1 and P_2 is reached, somewhat above RT, the transition rate is too slow to allow the change within the timescale of the experimental measurement. Only after several months of aging at RT does the transition to the equilibrium P_2 phase occur. In this scenario, the P_1 phase is the equilibrium phase for the higher concentrations within the temperature range from somewhat above RT (T_1) to 520 K (T_2), whereas the P_1 phase is the equilibrium phase for concentrations below about 3 at.% Sn. The P_2 phase is the equilibrium phase for the concentrations higher than 3 at.% Sn for temperatures below T_1 and above T_2. The P_1 phase is only kinetically stabilized at RT, and transforms over several months to the equilibrium P_2 phase for the higher Sn concentrations.

It should be emphasized that, whereas the above-mentioned description assumes a unique mechanism at the basis of the observed changes in IS shown in figures 2 and 3, i.e., changes in the Sn–Sn SRO atomic distribution, the possibility of a different origin behind the SIS (figure 3) cannot be ruled out (e.g., a local atomic displacement of the Sn atoms without changes in SRO could cause a SIS). The fact that both observed anomalies in IS occur only for the more concentrated samples and that the extrapolation of the high-temperature behaviour coincides, within uncertainties, with the RT LS after aging, however, is indicative of a unified mechanism being at the basis of the observed anomalies, and therefore we favour the description in terms of SRO changes as the most likely explanation of the experimental results.

4. Summary and conclusions

Careful measurements of the temperature-dependent LS in Ag–Sn alloys with Sn contents below the solubility limit reveal unexpected deviations from the smooth linear change of the

SODS, but only for the more concentrated alloys with above 3 at.% Sn. Samples that were aged for several months at RT initially showed hysteresis and a temperature-dependent LS that significantly deviates from the expected SODS behaviour. For these samples, a transformation to the expected slope is obtained at about $T \approx 520$ K accompanied by an increase in IS. Hysteresis in the temperature dependence of the LS is observed only in the first thermal cycle for the 4.0 and 8.0 at.% samples over the 300–500 K range, with the size of the effect being larger for the highest concentration. Upon cycling for the second time, the irreversibility disappears and the slope is as expected from a SODS linear dependence, but a transition at around $T \approx 520$ K persists. This transition produces a change in IS of $\Gamma/30$ which is equivalent to a shift in nuclear levels of 10^{-9} eV.

We attribute these changes to SRO effects where the Sn–Sn neighbour distribution changes due to a transition between two phases, P_1 and P_2, with the higher-temperature and higher-concentration phase P_2 having a SRO distribution corresponding to a slightly increased number of Sn–Sn neighbours. With the expectation that, due to entropy considerations, the high-temperature P_2 phase would have a more random distribution of Sn atoms, it is possible that the low-concentration and low-temperature P_1 phase undergoes an anti-clustering of its Sn impurities, as might be expected from strain effects caused by the increased size of the Sn atoms relative to the host Ag atoms.

Acknowledgments

We all wish to thank Y Khait, M Newville and A I Frenkel for very useful discussions. The research was supported by the Technion VPR fund and DOE Grant No DE-FG06-90ER 45425.

References

[1] Cai J and Yee Y Y 1996 *Phys. Rev.* B **54** 8398
[2] Saha T, Dasgupta I and Mookerjee A 1994 *Phys. Rev.* B **50** 13 267
[3] Martin C H and Singer S J 1991 *Phys. Rev.* B **44** 477
[4] Stern E A, Livins P and Zhe Zhang 1991 *Phys. Rev.* B **43** 8850
[5] Johnson R A 1990 *Phys. Rev.* B **41** 9717
[6] Shechter H, Stern E A, Yacoby Y, Brener R and Zhe Zhang 1989 *Phys. Rev. Lett.* **63** 1400
[7] Stern E A and Ke Zhang 1988 *Phys. Rev. Lett.* **60** 1872
[8] Mujibur-Rahman S M 1983 *J. Phys. F: Met. Phys.* **13** 303
[9] See, e.g.,
Frauenfelder H 1962 *The Mössbauer Effect* (New York: Benjamin)
[10] Greenwood N N and Gibb T C 1971 *Mössbauer Spectroscopy* (London: Chapman and Hall)
[11] Josephson B D 1960 *Phys. Rev. Lett.* **4** 341
[12] Maradudin A A, Flinn P A and Ruby J 1962 *Phys. Rev.* **126** 9
[13] Hanna S S and Preston R S 1965 *Phys. Rev.* **139** A722
[14] Goldanskii V I and Makarov E F 1968 *Chemical Applications of Mössbauer Spectroscopy* (New York: Academic)
[15] Singwi K S and Sjölander A 1960 *Phys. Rev.* **120** 1093
[16] Kohn W and Vosko S H 1960 *Phys. Rev.* **119** 912
[17] Haskel D, Shechter H, Stern E A, Newville M and Yacoby Y 1993 *Phys. Rev.* B **47** 14 032
[18] Khait Y L, Snapiro I B and Shechter H 1995 *Phys. Rev.* B **52** 9392
[19] Hansen M 1958 *Constitution of Binary Alloys* (New York: McGraw-Hill) p 52
[20] Margulies S and Ehrman J R 1961 *Nucl. Instrum. Methods* **12** 131
[21] Donaldson J D, Oteng R and Senior B J 1965 *Chem. Commun.* **24** 618
[22] Owen E A and Roberts E W 1939 *Phil. Mag.* **27** 294
[23] Bryukhanov V A, Delyagin N N and Shpinel V S 1965 *Sov. Phys.–JETP* **20** 55
[24] Balkashin O P and Chekin V V 1971 *Sov. Phys.–Solid State* **12** 2919

[25] Andreasen H, Damgaard S, Petersen J W and Weyer G 1983 *J. Phys. F: Met. Phys.* **13** 2077
[26] Garlipp W, Pfeiler W and Doppler T 1989 *Defect Diffusion Forum* **66–69** 497
[27] Tomizuka C T and Slifkin L 1954 *Phys. Rev.* **96** 610
[28] Stevens J G and Gettys W L (eds) 1981 *Isomer Shift Reference Scales* (Asheville, NC: Mössbauer Effect Data Center)
[29] Hondros E D and Seah M P 1977 *Int. Metall. Rev.* **222** 263
[30] Gas P and Bernardini J 1978 *Surf. Sci.* **72** 365
[31] Hentrich D, Faupel F and Hehenkamp T 1992 *Phil. Mag.* A **65** 207
[32] Mosig K, Wolff J, Kluin J-E and Hehenkamp T 1992 *J. Phys.: Condens. Matter* **4** 1447
[33] Haskel D, Stern E A and Shechter H 1998 *Phys. Rev.* B **57** 8034